British Journal of Multidisciplinary and Advanced Studies:
Mathematics, Statistics, Quantitative and Operations Research, 5(1),1-20, 2024
Print ISSN: 2517-276X
Online ISSN: 2517-2778
https://bjmas.org/index.php/bjmas/index
Published by the European Centre for Research Training and Development UK

Chemical Reaction and Nonlinear Rosseland Approximation Effects On Double-Diffusive MHD Sisko Nanofluid Flow Over a Nonlinear Stretching Sheet in A Porous Medium with Concentration-Dependent Internal Heat Source

Liberty Ebiwareme
Department of Mathematics, Rivers State University, Port Harcourt, Nigeria.

Kubugha Wilcox Bunonyo
Department of Mathematics/Statistics, Federal University Otuoke, Nigeria

doi: https://doi.org/10.37745/bjmas.2022.0415 Published February 07, 2024

Citation: Ebiwareme L. and Bunonyo K.W. (2024) Chemical Reaction and Nonlinear Rosseland Approximation Effects On Double-Diffusive MHD Sisko Nanofluid Flow Over a Nonlinear Stretching Sheet in A Porous Medium with Concentration-Dependent Internal Heat Source, British Journal of Multidisciplinary and Advanced Studies: Mathematics, Statistics, Quantitative and Operations Research5(1),1-19,

ABSTRACT: *This study investigates the two-dimensional magnetohydrodynamics laminar flow of a Sisko nanofluid over a nonlinear stretching sheet in a porous medium, considering chemical reactions, nonlinear Rosseland approximation, and an internal heat source based on concentration. The governing boundary layer equations and associated boundary conditions are transformed into non-dimensional form using appropriate variables. The resulting non-dimensional equations are solved using the modified Adomian decomposition technique, implemented with the symbolic computing software MATHEMATICA. The influence of various parameters, including Prandtl number, thermophoresis parameter, Brownian motion parameter, chemical reaction parameter, Sisko fluid parameters, heat source parameter, radiation parameter, Darcy number, mass Grashof number, magnetic field, and Grashof number, on the flow fields of velocity, temperature, and nanoparticles volume fractions is depicted through graphical representations. The study reveals that the velocity profile is accelerated by the first value of the Sisko fluid parameter and Darcy number, but it diminishes in the presence of a magnetic field and the second Sisko fluid parameter. The temperature profile decreases with an increment in the Prandtl number, while it improves in proportion to increases in the heat source, thermophoresis, Brownian motion, and radiation parameters respectively. Additionally, an increase in the chemical reaction parameter leads to an increase in the concentration profile of the fluid.*

KEYWORDS. Chemical reaction, MHD, thermal radiation, Sisko nanofluid, Double Diffusive

INTRODUCTION

Sisko Nanofluid is a cutting-edge and revolutionary product in the nanotechnology field. It is a specially designed fluid that incorporates nanoparticles to significantly enhance its thermal conductivity and heat transfer capabilities. This nanofluid has garnered significant attention across various industries, including automotive, aerospace, and electronics, owing to its remarkable performance and efficiency. Notably, one of the primary advantages of Sisko Nanofluid lies in its superior heat dissipation capabilities. The nanoparticles within the fluid serve as effective heat carriers, facilitating the efficient transfer of thermal energy in comparison to conventional fluids. As a result, this leads to reduced operating temperatures and improved performance of heat-generating systems, such as engines or electronic devices (Sisko and Zhang [1-2].

Moreover, Sisko Nanofluid demonstrates exceptional stability and suspension properties, guaranteeing the uniform dispersion of nanoparticles throughout the fluid. This effectively prevents the formation of agglomerates or sedimentation, which can impede flow and reduce overall efficiency. The inherent stability of the nanofluid also ensures long-term usage without significant degradation or loss of performance. Additionally, an important characteristic of Sisko Nanofluid is its compatibility with existing cooling systems. It can seamlessly integrate into conventional heat exchangers or radiators without the need for extensive modifications. This cost-effective quality makes it a viable solution for enhancing the heat dissipation capabilities of various equipment and systems Li et al. [3].

Numerous research studies have been conducted to assess the performance of Sisko Nanofluid. For instance, Zhang et al. [4] demonstrated its efficacy in reducing the operating temperature of electronic devices, thereby enhancing their reliability and lifespan. The study highlighted Sisko Nanofluid as a highly efficient and dependable solution for improving heat transfer and thermal management across diverse industries. Its outstanding performance, stability, and compatibility establish it as a preferred option for applications that require efficient heat dissipation. The multitude of research studies conducted on Sisko Nanofluid further substantiate its effectiveness and potential for widespread adoption. The effects of convective boundary conditions, partial slip conditions, and temperature-dependent thermal conductivity on the temperature and velocity profiles of forced convection in the flow of a Sisko nanofluid through a nonlinear stretching sheet were investigated by Munir et al. [5]. The study demonstrates that the thermal boundary layer thickness increases proportionally with the Eckert number. Hayat et al. [6] conducted an analysis on the heat transfer and hall effects of an electrically conducting incompressible Sisko fluid confined between two rotating disks using the homotopy analysis method. Khan et al. [7] performed a numerical study on mixed convective heat transfer to a Sisko fluid over a radially stretching sheet in the presence of convective boundary conditions. The research findings indicate that the buoyancy parameter has a more pronounced effect in the case of assisting flow compared to opposing flow. Furthermore, the analytical results obtained using the proposed method exhibit remarkable agreement when compared with the numerical results reported in the literature.

The problem of forced convective heat transfer to Sisko fluid flow past a stretching cylinder under the influence of variable thermal conductivity has been researched by Khan et al. [8-9]. The study revealed that the temperature and concentration profiles are larger in the case of flow past a cylinder compared to a flat plate, and the concentration profile decreases as the Brownian motion parameters increase. Malik et al. [10] implemented a numerical analysis of the characteristics of the Cattaneo-Christov double-diffusion model for Sisko fluid flow with velocity slip using the shooting technique combined with the Runge-Kutta-Fehlberg equation of order 4. By employing suitable transformations, the governing partial differential equations were converted into ordinary differential equations. The findings from the study demonstrated that the velocity decreases with the velocity slip parameter, and a decrease in temperature and concentration profiles was observed with larger relaxation times. Munir et al. [11] has conducted the investigation of forced convection on Sisko nanofluid over a stretching sheet, considering the effects of thermophoresis and Brownian motion on temperature and concentration. Ramanaiah [12] examined the impact of thermal radiation on convective heat and mass transfer of a Sisko nanofluid flowing past a stretching sheet. The study analysed the flow characteristics for various parameters, including the local Nusselt and Sherwood numbers. Mahmood et al. [13] addressed the combined effect of magnetohydrodynamics and radiation on nano Sisko fluid flow over a nonlinear stretching sheet. The findings indicated that the temperature profile increases with magnetic field, radiation, thermophoresis, and Brownian motion parameters.

Prasannakumara et al. [14] explored the flow and heat transfer of Sisko nanofluid over a nonlinear stretching sheet in the presence of magnetohydrodynamics and nonlinear thermal radiation. They found that the Nusselt and Sherwood numbers are higher for nonlinear stretching sheets, and nonlinear thermal radiation has a greater impact on temperature profiles. Abelman et al. [15] addressed the investigation of entropy generation in MHD and slip flow over a rotating porous disk with variable properties in the International Journal of Heat and Mass Transfer. Karim et al. [16] employed an explicit numerical technique to tackle the problem of unsteady hydromagnetic mixed convective nanofluid flow from an exponentially stretching sheet in porous media. Abdullah Al-Mamun et al. [17] examined the mathematical modelling of Sisko nanofluid flow through a nonlinear stretching sheet under the influence of magnetic field and thermal radiation. Arifuzzaman et al. [18] perused the investigation of the effect of chemical reaction and magnetohydrodynamics on the naturally convective flow through an oscillatory vertical porous plate, incorporating radiation absorption and heat transfer analysis. Ebiwareme et al. [19] tackled the influence of magnetohydrodynamics, nonlinear Rosseland approximation, chemical reaction, and concentration-based internal heat source on the heat and mass transfer flow of Sisko nanofluid through a nonlinear stretching sheet. Feroz Ahmed Soomro et al. [20] analysed the melting heat transfer of Sisko fluid over a moving surface with nonlinear thermal radiation using the collocation method. The results obtained revealed that the rate of heat and mass transfer is an increasing function, while the skin friction coefficient is a decreasing function of the melting parameter. Additionally, an increase in the thermal radiation effects enhances the heat and mass transfer rates. Furthermore, an increase in the power law index decreases velocity, temperature, and concentration distribution, while skin friction, heat, and mass transfer rates are enhanced due to an increase in the power law index.

The Adomian Decomposition Method (ADM), conceptualized by George Adomian in the 1980s, has become widely recognized for its efficiency in solving nonlinear differential and integral equations. Unlike traditional analytical methods, ADM transforms complex problems into series solutions, providing a powerful and flexible approach for addressing problems that do not have closed-form solutions. ADM decomposes a given equation into a series of terms, which are then solved iteratively. The method's strength lies in its ability to handle nonlinear equations without the need for linearization. Through the iterative process, ADM converges to an accurate solution, and it has been successfully applied to various linear and nonlinear problems in fields such as science and engineering. While other semi-analytical methods like the Homotopy Perturbation Method (HPM), Variational Iteration Method (VIM), and Optimal Homotopy Asymptotic Method (OHAM) offer approximate solutions to complex problems, ADM stands out due to its simplicity, applicability to a wide range of problems, and capability to handle non-polynomial terms directly. ADM requires minimal mathematical manipulations, making it accessible to researchers and practitioners with different levels of mathematical expertise. It has been successfully applied in physics, engineering, fluid dynamics, heat transfer, structural mechanics, and finance. Unlike some semi-analytical methods that require linearization, ADM excels in solving inherently nonlinear equations. However, it is important to note that ADM may have slow convergence for certain problems and lacks a rigorous error analysis framework. A comprehensive treatment of this innovative technique can be found in references [20-37].

In this research, our aim is to introduce a novel concentration-based internal heat source into the momentum equation, a concept that has not been previously explored. The study is structured as follows: Section one introduces the research along with an extensive review of relevant literature. Sections two and three present the formulation of boundary layer equations encompassing mass conservation, momentum, energy, and specie concentration. Sections four and onward detail the non-dimensionalization of governing equations and the fundamental approach to finding solutions. Section six delves into the application of the Adomian decomposition method to linearized equations, resulting in a recursive algorithm. Graphical representations of the effects of key parameters are presented in section seven, while the study's conclusions are summarized in section eight.

MATHEMATICAL FORMULATIONS

Consider the flow of a magnetohydrodynamic Sisko nanofluid generated by a stretched surface, influenced by nonlinear Rosseland approximation, chemical reaction, and an internal heat source based on concentration. The flow is oriented along the y-axis, and the velocity profile is described by a power law function, $U_0 = cx^s$. Temperature and concentration at the boundary layer are denoted as T_w and C_w, respectively, while away from the boundary layer, they are represented as T_∞ and C_∞. In the flow region, the magnetic field is assumed to be $\vec{B}_0 = (0, B_0, 0)$ as illustrated in Figure 1.

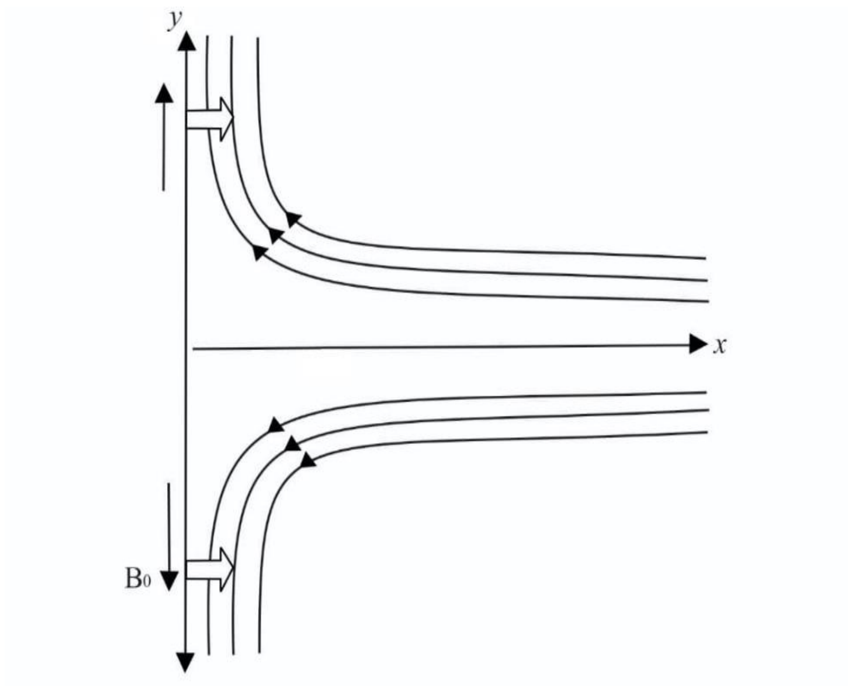

Figure 1. Flow configuration and co-ordinate system

The governing equations of continuity, momentum, energy, and specie concentration are provided as follows, building upon the studies conducted by Abdullah Al-Mamun et al. [18] and Ebiwareme et al. [19].

GOVERNING EQUATIONS

$$\frac{\partial u}{\partial x} + \frac{\partial v}{\partial y} = 0 \quad (1)$$

$$u\frac{\partial u}{\partial x} + v\frac{\partial u}{\partial y} = \frac{a}{\rho_f}\frac{\partial^2 u}{\partial y^2} + \frac{b}{\rho_f}\frac{\partial}{\partial y}\left(-\frac{\partial u}{\partial y}\right)^n - \frac{\sigma B_0^2}{\rho_f}u + g\beta_T(T - T_\infty) + g\beta_c(c - c_\infty) - \frac{v}{\kappa}u \quad (2)$$

$$u\frac{\partial T}{\partial x} + v\frac{\partial T}{\partial y} = \alpha\frac{\partial^2 T}{\partial y^2} + \tau\left[D_B\frac{\partial C}{\partial y}\frac{\partial T}{\partial y} + \frac{D_T}{T_\infty}\left(\frac{\partial T}{\partial y}\right)^2\right] - \frac{1}{\rho C_p}\frac{\partial q_r}{\partial y} + \frac{Q_0}{\rho_f}(c - c_\infty) \quad (3)$$

$$u\frac{\partial C}{\partial x} + v\frac{\partial C}{\partial y} = D_B\frac{\partial^2 C}{\partial y^2} + \frac{D_T}{T_\infty}\frac{\partial^2 T}{\partial y^2} - K_0(c - c_\infty) \quad (4)$$

The associated boundary conditions are as follows:

$$u(x,y) = U = cx^s, v(x,y) = 0, T = T_w, C = C_w \text{ at } y = 0$$

$$u \to 0, T \to T_\infty, C \to C_\infty \text{ as } y \to \infty \tag{5}$$

where (u, v) denote velocities in the coordinate axes, $a, b, n \geq 0$ are the material constants of the Sisko fluid, T represents temperature, C is the solid volume fraction of the fluid, ρ_f is the density of the fluid, σ denotes the electrical conductivity of the fluid, $\alpha = \frac{\kappa}{(\rho c)_f}$ is the thermal diffusivity of the fluid, D_B is the Brownian diffusion coefficient, D_T denotes the thermophoresis diffusion, g is the gravitational acceleration, $\tau = \frac{\rho_f C_p}{(\rho C)_f}$ is the ratio of effective heat capacity of the nanoparticles respectively.

In view of the Rosseland approximation, the radiative heat flux, q_r is expressible in the form.

$$q_r = -\frac{4\sigma^*}{3k^*}\frac{\partial T^4}{\partial y} = \frac{16\sigma^*}{3k^*}T_\infty^3\frac{\partial T}{\partial y} \tag{6}$$

where σ^* is the Stefan-Boltzmann constant and k^* is the mean absorption coefficient.

Upon simplification of Eq. (3) using Eq. (6), we have the equivalent form given as

$$u\frac{\partial T}{\partial x} + v\frac{\partial T}{\partial y} = \frac{\partial}{\partial y}\left[\left(\alpha + \frac{16\sigma^* T_\infty^3}{3k^*(\rho c)_f}\right)\frac{\partial T}{\partial y}\right] + \tau\left[D_B\frac{\partial C}{\partial y}\frac{\partial T}{\partial y} + \frac{D_T}{T_\infty}\left(\frac{\partial T}{\partial y}\right)^2\right] + \frac{Q_0}{\rho_f}(c - c_\infty) \tag{7}$$

NONDIMENSIONALIZATION OF GOVERNING EQUATIONS

To gain a deeper understanding of the physical problem, we simplify the governing equations by employing the following dimensionless variables.

$$\bar{x} = \frac{xU_0}{v}, \bar{y} = \frac{yU_0}{v}, \bar{u} = \frac{u}{U_0}, \bar{v} = \frac{v}{U_0}, \tau = \frac{tU_0^2}{v}, \ \theta = \frac{T - T_\infty}{T_w - T_\infty}, \phi = \frac{C - C_\infty}{C_w - C_\infty} \tag{8}$$

Upon substituting the above variables in Eq. (8) into Eqs. (1, 2, 4, 7), the expressions for the transformed velocity, temperature and nanoparticle volume fractions and dropping the bars are given as follows:

$$u\frac{\partial u}{\partial x} + v\frac{\partial u}{\partial y} = \frac{\partial^2 u}{\partial y^2}\left(A_1 + nA_2\left(\frac{\partial u}{\partial y}\right)^{n-1}\right) + Gr\theta + Gc\phi - \left(M + \frac{1}{Da}\right)u \tag{9}$$

$$\frac{\partial \theta}{\partial x} + \frac{\partial \theta}{\partial y} = \frac{1}{Pr}\left(1 + \frac{4R}{3}\right)\frac{\partial^2 \theta}{\partial y^2} + Nb\frac{\partial \phi}{\partial y}\frac{\partial \theta}{\partial y} + Nt\left(\frac{\partial \theta}{\partial y}\right)^2 + Q_0\phi \tag{10}$$

$$u\frac{\partial \phi}{\partial x} + v\frac{\partial \phi}{\partial y} = Nb\frac{\partial^2 \phi}{\partial y^2} + Nt\frac{\partial^2 \theta}{\partial y^2} - Kr\phi \tag{11}$$

subject to the appropriate boundary conditions given by

$$u = v = 1, \theta = 1, \phi = 0 \text{ at } y = 0$$
$$u = 0, \theta = 0, \phi = 0 \text{ at } y \to \infty \tag{12}$$

where $M = \frac{\sigma B_0^2 v}{\rho u_0^2}$ is the magnetic parameter, $Gc = \frac{g\beta_c(C_w - C_\infty)}{U_0^3}$ is mass Grashof number, $Gr = Gc = \frac{g\beta_T(T_w - T_\infty)}{U_0^3}$ is the Grashof number, $Da = \frac{\kappa U_0^2}{v^2}$ is Darcy number, $Pr = \frac{\rho c_p v}{\kappa}$ is Prandtl number, $R = \frac{\sigma T_\infty^3}{\kappa_e k}$ is radiation parameter, $Q_0 = \frac{\theta_0 v}{\rho C_p U_0^2}$ is the heat source parameter, $A_1 = \frac{a}{\rho v}, A_2 =$

Print ISSN: 2517-276X
Online ISSN: 2517-2778
https://bjmas.org/index.php/bjmas/index
Published by the European Centre for Research Training and Development UK

$\frac{bU_0^{2n-2}}{\rho \upsilon^n}$ are the Sisko fluid parameters, $Nb = \frac{D_B(C_w - C_\infty)}{\upsilon}$ is Brownian motion parameter, $Nt = \frac{D_T(T_w - T_\infty)}{\upsilon T_\infty}$ is the thermophoresis parameter, $K_r = \frac{\upsilon K_c(C_w - C_\infty)}{U_0^2}$ is the chemical reaction parameter

METHODOLOGY OF ADOMIAN DECOMPOSITION METHOD (ADM)

In this section, we will discuss the fundamental principles of the Adomian Decomposition method, as developed by the Armenian American mathematician, George Adomian. To illustrate its foundations, we will examine a nonlinear differential equation of the following form.

$$L[y(x)] + R[y(x)] + N[y(x)] = f(x) \quad (4)$$

where L is an invertible highest order derivative, R is the remainder of the linear term, $N(y)$ is a nonlinear term and $f(x)$ is the source term.
Rewriting Eq. (4) in operator form, we have the expression.

$$L[y(x)] = f(x) - R[y(x)] - N[y(x)] \quad (5)$$

Applying the inverse operator L^{-1} to both sides of Eq. (5), we obtain the form as

$$L^{-1}(Ly(x)) = L^{-1}\big(f(x)\big) - L^{-1}(Ry(x)) - L^{-1}(Ny(x)) \quad (6)$$

where $L^{-1}(.) = \int_0^x \int_0^x \int_0^x \int_0^x \dots\dots\dots\dots \int_0^x (.)dxdx\,dxdx \dots\dots\dots\dots dx$

$$y(x) = \varphi_0(x) + g(x) - L^{-1}R[y(x)] - L^{-1}N[y(x)] \quad (7)$$

where $\mathrm{g}(x)$ is the term obtained from integrating the source term from the given boundary conditions. Now rewriting the solution and nonlinear terms as decomposition series of the form

$$y(x) = \sum_{n=0}^{\infty} y_n(x),\ N[y(x)] = \sum_{n=0}^{\infty} A_n(x), \quad (8)$$

where the $A_n'^s$ are the so-called Adomian polynomials obtained using the formula

$$A_k = \frac{1}{k!}\frac{\partial^k}{\partial \lambda^k}[N(\sum_{n=0}^{\infty} y_{n\lambda^n})]_{\lambda=0}, k = 0,1,2 \dots \quad (9)$$

Putting Eq. (8) into Eq. (7), we obtain the solution in the form of a decomposition series as follows.

$$\sum_{n=0}^{\infty} y_n(x) = y(x) = \varphi_0(x) + g(x) - L^{-1}R(\sum_{n=0}^{\infty} y_n(x)) - L^{-1}N(\sum_{n=0}^{\infty} A_n(x)) \quad (10)$$

where $y_0(x) = \varphi_0(x) + g(x)$ is the zeroth component of the solution, $y_n(x)$. The subsequent members of the series are obtained recursively using the algorithm.

$$y_{k+1} = -L^{-1}R\big(y_k(x)\big) - L^{-1}(A_k(x)), \qquad k \geq 0 \quad (11)$$

Then exact solution of the problem is obtained by taking the limit of the recursive scheme.

$$y(x) = \lim_{n\to\infty} \sum_{k=0}^{n} y_k(x) \quad (12)$$

MATHEMATICAL ANALYSIS USING ADM

Rewriting Eqs. (9-11) in an equivalent operator form as follows.

$$\left(A_1 + nA_2\left(\frac{\partial u}{\partial y}\right)^{n-1}\right)\frac{\partial^2 u}{\partial y^2} = u\frac{\partial u}{\partial x} + v\frac{\partial u}{\partial y} - Gr\theta + Gc\phi + \left(M + \frac{1}{Da}\right)u \quad (13)$$

$$\frac{1}{Pr}\left(1+\frac{4R}{3}\right)\frac{\partial^2\theta}{\partial y^2}=\frac{\partial\theta}{\partial x}+\frac{\partial\theta}{\partial y}-Nb\frac{\partial\phi}{\partial y}\frac{\partial\theta}{\partial y}-Nt\left(\frac{\partial\theta}{\partial y}\right)^2-Q_0\phi \tag{14}$$

$$Nb\frac{\partial^2\phi}{\partial y^2}=u\frac{\partial\phi}{\partial x}+v\frac{\partial\phi}{\partial y}-Nt\frac{\partial^2\theta}{\partial y^2}+Kr\phi \tag{15}$$

Using the stream function formulation, ψ in terms of velocity is given as.

$$u=\frac{\partial\psi}{\partial y}\ ,v=-\frac{\partial\psi}{\partial x} \tag{16}$$

Using Eq. (16), mass conservation equation is automatically satisfied, thus we have only three equations to be solved.
Rewriting Eqs. (13-15) in operator form as follows.

$$L_1u(x,y)=\frac{1}{\left(A_1+nA_2\left(\frac{\partial u}{\partial y}\right)^{n-1}\right)}\left[u\frac{\partial u}{\partial x}+v\frac{\partial u}{\partial y}-Gr\theta+Gc\phi+\left(M+\frac{1}{Da}\right)u\right] \tag{17}$$

$$L_2\theta(x,y)=\frac{1}{\frac{1}{Pr}\left(1+\frac{4R}{3}\right)}\left[\frac{\partial\theta}{\partial x}+\frac{\partial\theta}{\partial y}-Nb\frac{\partial\phi}{\partial y}\frac{\partial\theta}{\partial y}-Nt\left(\frac{\partial\theta}{\partial y}\right)^2-Q_0\phi\right] \tag{18}$$

$$L_3\phi(x,y)=\frac{1}{Nb}\left[u\frac{\partial\phi}{\partial x}+v\frac{\partial\phi}{\partial y}-Nt\frac{\partial^2\theta}{\partial y^2}+Kr\phi\right] \tag{19}$$

where the differential operators, L_1, L_2 and L_3 are given by $L_1=L_2=L_3=\frac{\partial^2}{\partial y^2}$ respectively. Assuming that the inverse of the operator, $L_i(i=1,2)$ exists and is integrated from 0 to y as follows.

$$L_1^{-1}=L_2^{-1}=L_3^{-1}=\int_0^y\int_0^y(.)dydy \tag{20}$$

From Eqs. (17-19), the nonlinear terms are generated using the recursive algorithm or scheme known as Adomian polynomials.

$$A_n=\frac{1}{n!}\left[\frac{d^n}{d\lambda^n}\left(\sum_{k=0}^{n}\lambda^n u_k\right)\right]_{\lambda=0},n=0,1,2,3 \tag{21}$$

The solutions of Eqs. (17-19) is obtained using the following recursive schemes.

$$u_{n+1}(x,y)=L^{-1}\left(\sum_{n=0}^{n}A_n\right),\theta_{n+1}(x,y)=L^{-1}\left(\sum_{n=0}^{n}B_n\right),\phi_{n+1}(x,y)=L^{-1}\left(\sum_{n=0}^{n}C_n\right) \tag{22}$$

Operating both sides of Eqs. (17-19) with the inverse as defined in Eq. (20) and applying the given boundary conditions, we have.

$$\begin{gathered}u(x,y)=u(0)+yu'(0)+L_1^{-1}(N_1u)\\ \theta(x,y)=\theta(0)+y\theta'(0)+L_2^{-1}(N_2u)\\ \phi(x,y)=\phi(0)+y\phi'(0)+L_3^{-1}(N_3u)\end{gathered} \tag{23}$$

where the nonlinear terms, N_is are defined as follows.

$$N_1(u)=\frac{1}{\left(A_1+nA_2\left(\frac{\partial u}{\partial y}\right)^{n-1}\right)}\left[u\frac{\partial u}{\partial x}-Gr\theta+Gc\phi+\left(M+\frac{1}{Da}\right)u\right]$$

$$N_2(\theta)=\frac{1}{\frac{1}{Pr}\left(1+\frac{4R}{3}\right)}\left[\frac{\partial\theta}{\partial x}+\frac{\partial\theta}{\partial y}-Nb\frac{\partial\phi}{\partial y}\frac{\partial\theta}{\partial y}-Nt\left(\frac{\partial\theta}{\partial y}\right)^2-Q_0\phi\right] \tag{24}$$

Print ISSN: 2517-276X
Online ISSN: 2517-2778
https://bjmas.org/index.php/bjmas/index
Published by the European Centre for Research Training and Development UK

$$N_3(\phi) = \frac{1}{Nb}\left[u\frac{\partial \phi}{\partial x} - Nt\frac{\partial^2 \theta}{\partial y^2} + Kr\phi\right]$$

Then the flow profiles, $u(x,y), \theta(x,y)$ and $\phi(x,y)$ are expressed in the form.

$$u(x,y) = \sum_{n=0}^{\infty} u_m(x,y), u(x,y) = \sum_{n=0}^{\infty} u_m = u_0 + L^{-1}(N_1 u)$$
$$\theta(x,y) = \textstyle\sum_{n=0}^{\infty} \theta_m(x,y), \theta(x,y) = \sum_{n=0}^{\infty} \theta_m = \theta_0 + L^{-1}(N_1\theta) \quad (25)$$
$$\phi(x,y) = \sum_{n=0}^{\infty} \phi_m(x,y), \phi(x,y) = \sum_{n=0}^{\infty} \phi_m = \phi_0 + L^{-1}(N_1\phi)$$

The nonlinear terms of $u(x,y), \theta(x,y)$ and $\phi(x,y)$ are expressed as a series of the form as follows.

$$N_1\left(u, \frac{\partial u}{\partial x}\right) = \sum_{m=0}^{\infty} B_m = u\frac{\partial u}{\partial x} \Longrightarrow B_0 = u_0 u_{0x}, B_1 = u_0 u_{1x} + u_1 u_{0x}$$
$$N_3\left(\frac{\partial \phi}{\partial y}, \frac{\partial \theta}{\partial y}\right) = \sum_{m=0}^{\infty} C_m = \frac{\partial \phi}{\partial y}\frac{\partial \theta}{\partial y} \Longrightarrow C_0 = \phi_{0y}\theta_{0y}, C_1 = \phi_{0y}\theta_{1y} + \phi_{1y}\theta_{0y}$$
$$N_4\left(\frac{\partial \theta}{\partial y}, \frac{\partial \theta}{\partial y}\right) = \sum_{m=0}^{\infty} D_m = \left(\frac{\partial \theta}{\partial y}\right)^2 \Longrightarrow D_0 = \left(\theta_{0y}\right)^2, D_1 = 2\theta_{0y}\theta_{1y}$$
$$N_5\left(u, \frac{\partial \phi}{\partial x}\right) = \sum_{m=0}^{\infty} E_m = u\frac{\partial \phi}{\partial x} \Longrightarrow E_0 = u_0\phi_{0x}, E_1 = u_0\phi_{1x} + u_1\phi_{0x}$$

Using Eq. (25), the zeroth order iterative solution gives the expressions.

$$u_0(x,y) = 1 + \delta_1 y, \theta_0(x,y) = 1 + \delta_2 y, \phi_0(x,y) = \delta_3 y \quad (26)$$

The recursive algorithm valid for $m \geq 0$ for the flow distributions under the impressions of the boundary conditions is given by.

$$u_{m+1}(x,y) = L_1^{-1}\left[\frac{1}{\left(A_1 + nA_2\left(\frac{\partial u}{\partial y}\right)^{n-1}\right)}\left[B_m + \left(M + \frac{1}{Da}\right)u_m - Gr\theta_m + Gc\phi_m\right]\right] \quad (27)$$
$$\theta_{m+1}(x,y) = L_2^{-1}\left[\frac{1}{\frac{1}{Pr}\left(1 + \frac{4R}{3}\right)}\left[\frac{\partial \theta_m}{\partial x} + \frac{\partial \theta_m}{\partial y} - NbB_m - NtC_m - Q_0\phi_m\right]\right] \quad (28)$$
$$\phi_{m+1}(x,y) = L_3^{-1}\left[\frac{1}{Nb}\left(D_m - Nt\frac{\partial^2 \theta_m}{\partial y^2} + Kr\phi_m\right)\right] \quad (29)$$

For the complete solution of the problem, the components, $u_m(x,y), \theta_m(x,y)$ and $\phi_m(x,y)$ are obtained by applying the boundary conditions in Eq. (12) to determine the constants, $\delta_1, \delta_2, \delta_3, \alpha_1, \alpha_2$. However, the accuracy of the problem is dependent on the consideration of more solution terms in the recursive algorithm.

Using the recursive relations, the three-term approximate solutions of the flow profiles take the form.

$$u(x,y) = \sum_{m=0}^{\infty} u_m(x,y) = u_0(x,y) + u_1(x,y) + u_2(x,y) + \cdots$$
$$\theta(x,y) = \sum_{m=0}^{\infty} \theta_m(x,y) = \theta_0(x,y) + \theta_1(x,y) + \theta_2(x,y) + \cdots \quad (30)$$
$$\phi(x,y) = \sum_{m=0}^{\infty} \phi_m(x,y) = \phi_0(x,y) + \phi_1(x,y) + \phi_2(x,y) + \cdots$$

RESULTS AND DISCUSSION

The reduced nonlinear partial differential equations in Eqs. (9-11) along with associated boundary conditions Eq. (12) is addressed using a semi-analytical approach within the framework of the Adomian decomposition method. Various influential parameters, such as Prandtl number (Pr), thermophoresis parameter (Nt), Brownian motion parameter (Nb), chemical reaction parameter (Kr), Sisko fluid parameters (A_1, A_2), heat source parameter (Q_0), radiation parameter (R), Darcy number (Da), mass Grashof number (G_m), magnetic field (M), and Grashof number (Gr), are systematically examined. The impact of these parameters on the flow fields, including velocity, temperature, and nanoparticles volume fractions, is illustrated through Figures $2-15$. For computational purposes, we take the values of the physical parameters as follows: $Da = 1.60, G_m = 2.00, M = 1.20, A_1 = 1.20, A_2 = 0.60, Pr = 2.0, R = 0.30, Q = 1.40, Le = 8.00, Nt = 0.1, Nb = 0.1, Kr = 0.50$.

5.1 Dimensionless velocity profile

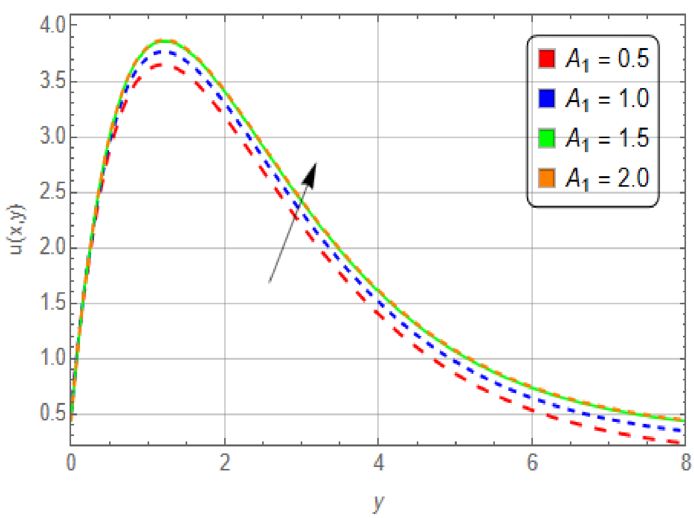

Figure 2. Effect of Sisko parameter on velocity profile

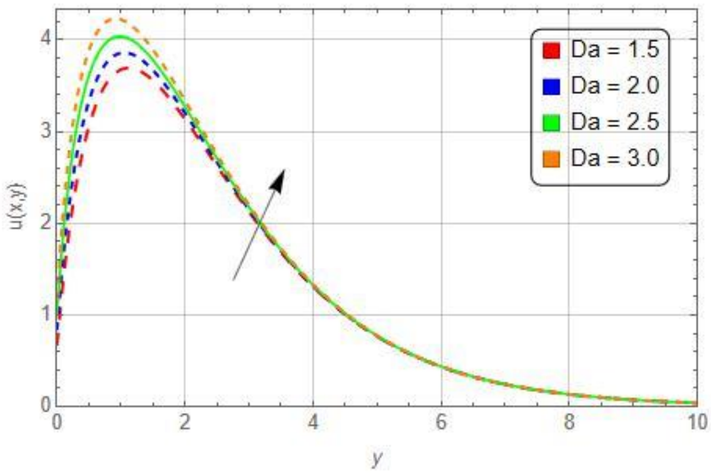

Figure 3. Effect of Darcy number on velocity profile

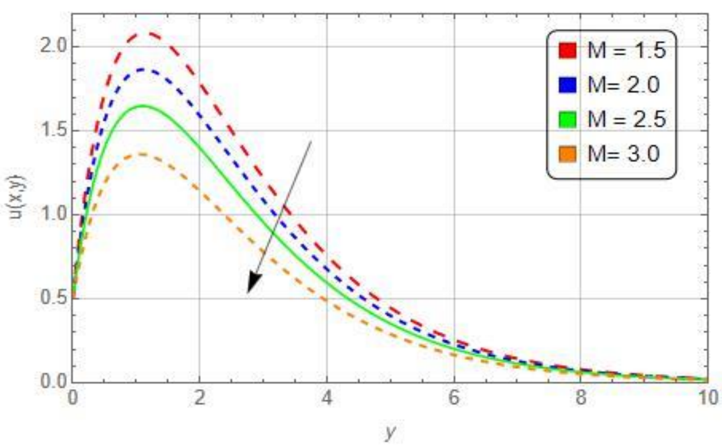

Figure 4. Effect of Hartmann number on velocity profile.

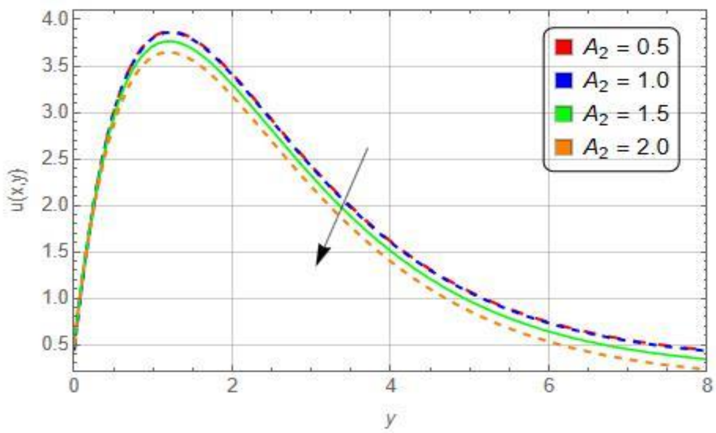

Figure 5. Effect of Sisko parameter on velocity profile.

5.2 Dimensionless Temperature profile

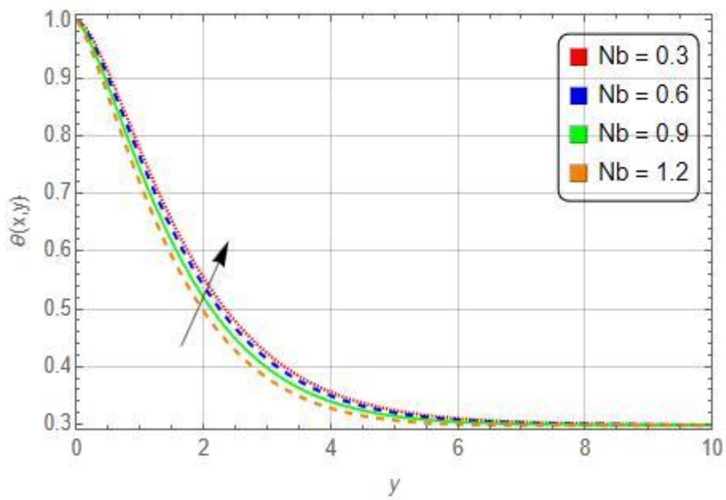

Figure 6. Effect on Brownian motion on temperature profile

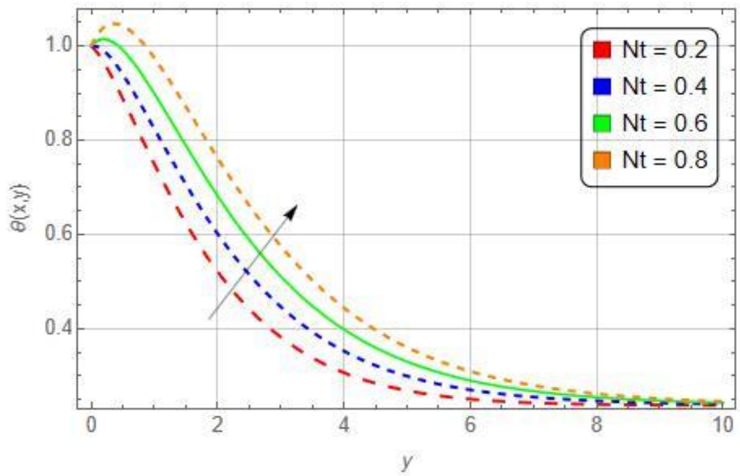

Figure 7. Impact of Thermophoresis on temperature profile

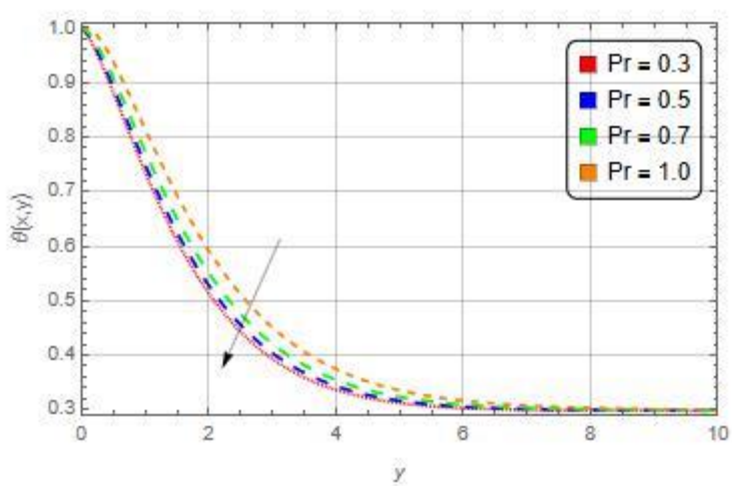

Figure 8. Effect of Prandtl number on temperature profile

Print ISSN: 2517-276X
Online ISSN: 2517-2778
https://bjmas.org/index.php/bjmas/index
Published by the European Centre for Research Training and Development UK

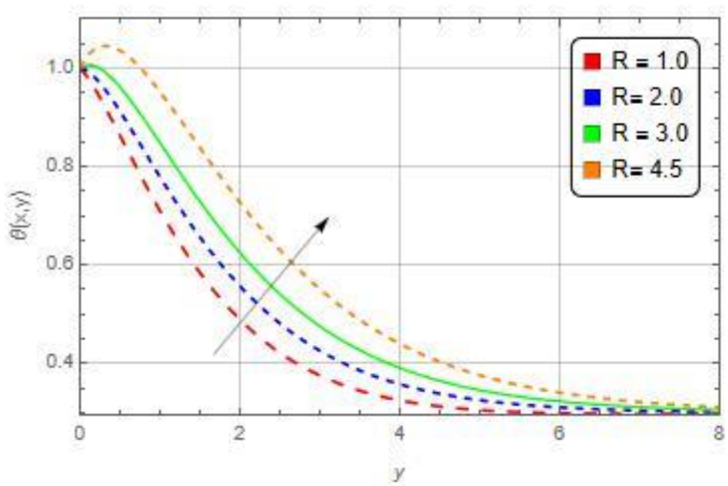

Figure 9. Influence of radiation parameters on temperature profile

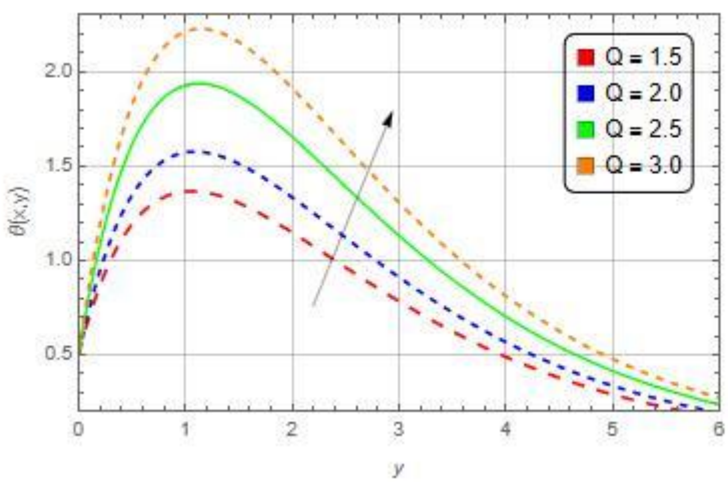

Figure 10. Effect of heat source on temperature profile

5.3 Dimensionless Nanoparticles volume fraction profiles

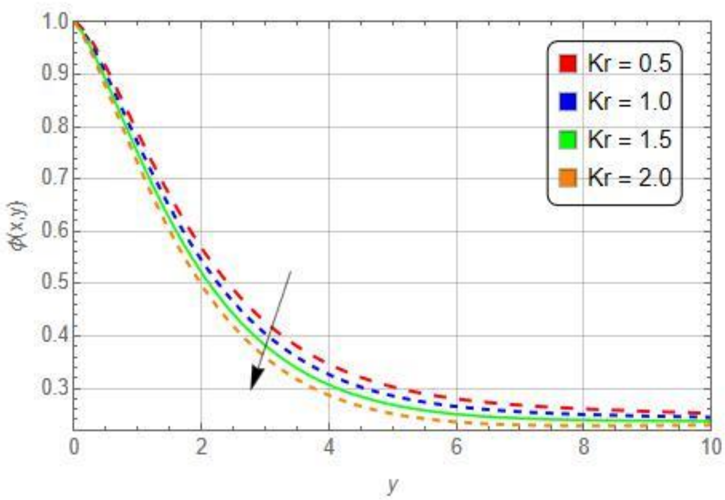

Figure 11. Effect of chemical reaction on concentration profile

CONCLUDING REMARKS

Theoretical investigation is undertaken on the dynamics of a chemically reactive double diffusive magnetohydrodynamic Sisko nanofluid flowing through a porous medium over a nonlinear stretching sheet, influenced by nonlinear thermal radiation and an internal heat source based on concentration. The governing model equations are transformed through nondimensionalization and are subsequently solved semi-analytically using the recursive Adomian decomposition scheme. The study yields the following conclusions based on our results.

- Acceleration of the velocity profile was observed with an increase in both the first Sisko field parameter and the Darcy number.
- The velocity profile diminishes as a result of the second Sisko fluid parameter and the magnetic field parameter.
- The thermophoresis parameter, Brownian motion parameter, heat source, and radiation parameter all lead to an increase in the temperature distributions.
- Temperature profiles plummeted as the Prandtl number increased.
- The concentration profile of nanoparticles exhibits deceleration in the presence of the chemical reaction parameter.

REFERENCES

[1] Sisko, J., & Zhang, D. (2014). Heat transfer and flow characteristics of shear-thinning nanofluids. International Journal of Heat and Mass Transfer, 77, 115-123.

[2] Sisko, J., & Zhang, D. (2016). A review on the rheological behaviour of shear-thinning nanofluids. Journal of Nanofluids, 5(1), 1-17

[3] Li, J., et al. (2018). Thermal conductivity enhancement of Sisko nanofluid with graphene nanoplatelets. International Journal of Heat and Mass Transfer, 121, 1-9.

[4]. Zhang, Y., et al. (2019). Experimental investigation on the thermal performance of Sisko nanofluid for electronic cooling applications. Applied Thermal Engineering, 150, 161-168

[5] Munir A, Shahzad A, Khan M. (2014). Forced convective heat transfer in boundary layer flow of Sisko fluid over a nonlinear stretching sheet. PLOS ONE 9(6): e100056. https://doi.org/10.1371/journal.pone.0100056

[6] Hayat T, Maqbool K, Asghar S. (2009). Hall and heat transfer effects the steady flow of a Sisko fluid. A Journal of Physical Sciences 64(12): 769-782. https://doi.org/10.1515/zna-2009-1201

[7] Khan M, Malik R, Munir A. (2015). Mixed convective heat transfer to Sisko fluid over a radially stretching sheet in the presence of convective boundary conditions. AIP Advances 5: 087178. https://doi.org/10.1063/1.4929832

[8] Khan M, Malik R. (2015). Forced convective heat transfer to Sisko fluid flow past a stretching cylinder. AIP Advances 5: 127202. https://doi.org/10.1063/1.4937346

[9] Khan M, Malik R, Hussain M. (2016). Nonlinear radiative heat transfer to stagnation-point flow of Sisko fluid past a stretching cylinder AIP Advances 6: 055315. https://doi.org/10.1063/1.4950946

[10] Malik R, Khan M, Shafiq A, Mushtaq M, Hussain M. (2017). An analysis of Cattaneo-Christov double diffusion model for Sisko fluid flow with velocity slip. Results in Physics 7: 2458-2469. https://doi.org/10.1016/j.rinp.2017.03.027

[11] Khan M, Malik R, Munir A, Khan WA. (2015). Flow and heat transfer to Sisko nanofluid over a nonlinear stretching sheet. PLOS ONE 10(5): e0125683. https://doi.org/10.1371/journal.pone.0125683

[12] Ramanaiah GV, Babu MS, Lavanya ML. (2016). Convective heat and mass transfer flow of Sisko nanofluid past a nonlinear stretching sheet with thermal radiation. International Refereed Journal of Engineering and Science 5(2): 17-37. https://doi.org/10.1166/jon.2019.1620

[13] Mahmood T, Iqbal Z, Ahmed J, Shahzad A, Khan M. (2017). Combined effects of magnetohydrodynamics and radiation on nano Sisko fluid towards a nonlinear stretching sheet. Results in Physics 7: 2458-2469. https://doi.org/10.1016/j.rinp.2017.05.003

[14] Prasannakumara BC, Gireesha BJ, Krisnamurthy MR, Kumar KG. (2017). MHD flow and nonlinear radiative heat transfer of Sisko nanofluid over a nonlinear stretching sheet. Informatics in Medicine Unlocked 9: 123-132. https://doi.org/10.1016/j.imu.2017.07.006

[15] Rashidi MM, Kavyani N, Abelman S. (2013). Investigation of entropy generation in MHD and slip flow over a rotating porous disk with variable properties. International Journal of

Heat and Mass Transfer 70: 892917. https://doi.org/10.1016/j.ijheatmasstransfer.2013.11.058

[16] Bég OA, Khan MS, Karim I, Alam MM, Ferdows M. (2014). Explicit Numerical study of unsteady hydromagnetic mixed convective nanofluid flow from an exponentially stretching sheet in porous media. Applied Nanoscience 4(8): 943-957. https://doi.org/10.1007/s13204-013-0275-0

[17] Arifuzzaman SM, Khan MS, Mehedi MFU, Rana BMJ, Biswas P, Ahmed SF. (2018), Chemically reactive and naturally convective high speed MHD fluid flow through an oscillatory vertical porous plate with heat and radiation absorption effect. Engineering Science and Technology, an International Journal 21(2): 215-228. https://doi.org/10.1016/j.jestch.2018.03.004.

[18] Abdullah Al-Mamun, S. M., Arifuzzaman, S. K., Reza, E. R., Pronab Biswas M. D., Shakhaoath, K. (2019). Computational Modelling on MHD Radiative Sisko Nanofluids Fow through a nonlinearly stretching sheet. International Journal of Heat and Technology, Vol. 37, No. 1, pp. 285-295.

[19] Ebiwareme, L., Esekhaigbe, E., Bunonyo, K. W., Uka, U. A. (2023) Magnetohydrodynamics nonlinear radiative heat and mass transfer flow of Sisko nanofluid through a nonlinear stretching sheet in the presence of chemical reaction. Journal of Advances in Mathematics and Computer Science, Volume 38, Issue 11, Pages 72-86.

[20] Soomro, F., Usman, M., Haq, R., & Wang, W. (2018). Melting heat transfer analysis of Sisko fluid over a moving surface with nonlinear thermal radiation via Collocation method. International Journal of Heat and Mass Transfer. https://doi.org/10.1016/J.IJHEATMASSTRANSFER.2018.05.099.

[21] Adomian, G. (1988). A review of the Decomposition Method in applied mathematics. Journal of Mathematical Analysis and Applications, 135(2), 501-544.

[22] Ebiwareme, L. (2021). Application of Semi-analytical iteration techniques for the numerical solution of linear and nonlinear Differential Equations. International Journal of Mathematics Trends and Technology, Volume 67, issue 2, 146-158.

[23] Ebiwareme, L., Da-Wariboko Y.A. (2021). Modified Adomian decomposition method and Pade approximant for the Numerical approximation of the deterrence model in society. The International Journal of Engineering Science, Volume 16, Issue 7, Series 1, pages 01-12, 2021.

[24] Ebiwareme, L. (2022). A comparative study between semi-analytical iterative schemes for the reliable treatment of coupled nonlinear partial differential equations. International Journal of Innovation Engineering and Science Research. Volume 6, Issue 1, January-February 2021

[25] Ebiwareme, L. (2022). Analytical solution of the dynamics of atmospheric C02 using LADM-Pade approximation approach, International Journal of Trend in Scientific Research and Development, Volume 6, Issue 2, January-February 2022.

[26] Wazwaz, A. M. (2009). A First Course in Integral Equations. World Scientific.

[27] Abbasbandy, S. (2006). The application of Adomian decomposition method for a reliable treatment of the nonlinear Klein-Gordon equation. Applied Mathematics and Computation, 173(1), 485-497.

[28] Ebiwareme, L., Akpodee, R. E., Ndu, R. I. (2022). An application of LADM-Pade approximation for the analytical solution of the SIR infectious Disease Model. International Journal of Innovation Engineering and Science Research. Volume 6, Issue 2, March-April 2022.

[29] Ebiwareme, L. (2022). Analytical study of the Hepatitis E Virus Model (HEV) vis Hybrid semi-analytical Laplace Transformation Adomian decomposition method. Volume 5, Issue 1, Jan-Feb 2022.

[30] Ebiwareme, L., Bunonyo, K. W., Davies, O. A. (2023). Heat transfer analysis of magnetohydrodynamics fluid flow past an infinite vertical porous plate in the presence of suction: the Adomian Decomposition Method Approach. American Journal of Engineering Research, Volume 12, issue-2, pp-146-160

[31] Ebiwareme, L., Bunonyo, K. W. (2023). Analytical investigation of MHD Casson fluid flow past an inclined semi-infinite porous plate with radiation absorption and magnetic field effects. International Research Journal of Innovations in Engineering and Technology. Volume 7, issue 3, pp 36-49, March 2023.

[32] Adomian, G. (1994). Solving Frontier Problems of Physics: The Decomposition Method. Boston: Kluwer Academic Publishers.

[33] Abassy, T. A., & El-Danaf, T. S. (2005). A Comparative Study between Adomian Decomposition Method and Homotopy Perturbation Method. Applied Mathematics and Computation, 170(1), 542-551.

[34] Ebiwareme, L., Bunonyo, K. W., O.A. Davies (2023). Analytical Solution for Heat and Mass Transfer of two-phase Nanofluid Flow with Magnetic Field in a rotating System using Adomian Decomposition Method. International Journal of Scientific and Innovative Mathematical Research, Volume 11, Issue 2, PP. 1-16.

[35] Ebiwareme, L., Bunonyo, K. W., Tasie, N. K. (2023). On the Adomian Decomposition Method for the Analytical Modelling of Steady State Condensation Film in an Inclined Rotating Disk. International Journal of Advances in Applied Mathematics and Mechanics, 10(3), 78-88.

[36] Ebiwareme, L., Bunonyo, K.W., Davies, O. A. (2023). Comparison of Adomian decomposition method with Differential transformation method for unsteady MHD flow and heat transfer over a stretching/Shrinking permeable sheet with Ohmic heating. African Journal of Mathematics and Statistics Studies, Volume 6, Issue 3, 70-85.

[37] Abbasbandy, S. (2006). The Application of Homotopy Analysis Method to Nonlinear Equations Arising in Heat Transfer. Physics Letters A, 360(1), 109-113.

NOMENCLATURE

British Journal of Multidisciplinary and Advanced Studies:
Mathematics, Statistics, Quantitative and Operations Research, 5(1),1-20, 2024
Print ISSN: 2517-276X
Online ISSN: 2517-2778
https://bjmas.org/index.php/bjmas/index
Published by the European Centre for Research Training and Development UK

u, v	Velocity components along x and y
x, y	Cartesian coordinates
U_0	Uniform velocity
A_1, A_2	Sisko fluid parameters
C_p	Specific heat capacity at constant pressure
Da	Darcy number
D_B	Brownian diffusion coefficient
D_T	Thermophoresis diffusion coefficient
Gr	Grashof number
G_m	modified Grashof number
K	permeability of the porous medium
k^*	mean absorption coefficient.
Le	Lewis number
σ^*	Stefan-Boltzmann constant.
Nb	the Brownian parameter
Nt	the thermophoresis parameter
Q	Heat source parameter
Pr	Prandtl number
M	Magnetic field
R	Radiation parameter
B_0	Induced magnetic field.
q_r	Unidirectional radiative heat flux
T	Fluid temperature
T_w	Uniform wall temperature
T_∞	Ambient temperature
C_w	Concentration of the walls
C_∞	Ambient concentration
n	Power law index
N_{ux}	Local Nusselt number
S_{hx}	Local Sherwood number
a, b	Material constants of the fluid

Greek Letters

α	Fluid thermal diffusivity
ρ_f	Fluid density
σ	Electrical conductivity of the fluids
κ	Thermal conductivity
θ	Dimensionless temperature of the fluid
ϕ	Dimensionless Concentration
η	Similarity variable
υ	Kinematic viscosity

ψ	Stream function
τ	Ratio of the effective heat capacity of the nanoparticles to heat capacity of the fluid.